molecular pharmaceutics

Article

pubs.acs.org/molecularpharmaceutics

Angiopep-2 and Activatable Cell-Penetrating Peptide Dual-Functionalized Nanoparticles for Systemic Glioma-Targeting Delivery

Huile Gao, Shuang Zhang, Shijie Cao, Zhi Yang, Zhiqing Pang, and Xinguo Jiang*

Key Laboratory of Smart Drug Delivery (Fudan University), Ministry of Education, Department of Pharmaceutics Sciences, School of Pharmacy, Fudan University, 826 Zhangheng Road, Shanghai 201203, China

Supporting Information

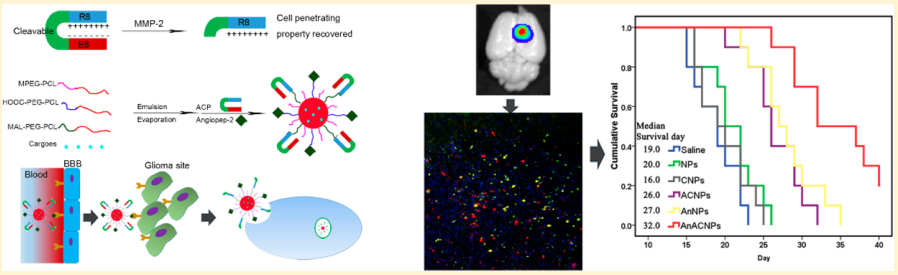

ABSTRACT: Gliomas are hard to treat because of the two barriers involved: the blood−brain barrier and blood−tumor barrier. In this study, a dual-targeting ligand, angiopep-2, and an activatable cell-penetrating peptide (ACP) were functionalized onto nanoparticles for glioma-targeting delivery. The ACP was constructed by conjugating RRRRRRRR (R8) with EEEEEEEE through a matrix metalloproteinase-2 (MMP-2)-sensitive linker. ACP modification effectively enhanced the C6 cellular uptake because of the high expression of MMP-2 on C6 cells. The uptake was inhibited by batimastat, an MMP-2 inhibitor, suggesting that the cell-penetrating property of the ACP was activated by MMP-2. By combining the dual-targeting delivery effect of angiopep-2 and activatable cell-penetrating property of the ACP, the dual-modified nanoparticles (AnACNPs) displayed higher glioma localization than that of single ligand-modified nanoparticles. After loading with docetaxel, a common chemotherapeutic, AnACNPs showed the most favorable antiglioma effect both in vitro and in vivo. In conclusion, a novel drug delivery system was developed for glioma dual targeting and glioma penetrating. The results demonstrated that the system effectively targeted gliomas and provided the most favorable antiglioma effect.

KEYWORDS: *glioma, systemic targeted delivery, activatable cell-penetrating peptide, angiopep-2*

1. INTRODUCTION

Cancer is one of the leading threats for human health. Nanoparticles (NPs) are widely used to increase drug delivery to tumors because of the heightened permeability and retention (EPR) effect.[1,2] However, because of the lack of vessels, reaching tumor cells is difficult for NPs or drugs as a result of their poor penetration ability. Cell-penetrating peptides (CPPs) could be anchored onto the surface of NPs to enhance their tissue permeability.[3,4] However, applying CPPs is hampered by the poor selectivity between neoplastic and nonneoplastic cells.[5,6] To circumvent this problem, CPPs could be shielded by poly(ethylene glycol) (PEG) or anionic peptides in the blood,[7−9] which could detach in the tumor under certain circumstances, boosting the penetration ability of CPPs.

Gliomas are difficult to treat because of the complex microenvironment. The blood−brain barrier (BBB) is considered as the first barrier that restricts the distribution of drugs from blood to brain, owing to the tight junction of endothelial cells and various efflux transporters on the BBB.[10−12] Although the BBB is compromised in brain tumors,[13] the compromise is restricted to the tumor bed. The BBB is integrated in the invasive part of brain tumors, particularly in the part distanced from the tumor bed.[14] Another barrier is the blood−tumor barrier (BTB), which restricts the distribution of drugs from blood to tumor because of the high internal pressure of the tumor.[15,16] The BTB of brain tumors is tighter than the BTB of peripheral tumors regarding the transendothelial fenestrations, transporter expression, and interendothelial cell gaps.[17,18]

Dual-targeting delivery systems have effectively circumvented the BBB and BTB and specifically delivered drugs to glioma sites.[19,20] However, the poor penetration ability still hampered the treatment outcome. In this study, we combined the benefit of a dual-targeting delivery system and CPPs to effectively deliver cargoes to glioma cells and to further improve the glioma treatment (Figure 1).

To enable the delivery system to target both the BBB and glioma, the ligand needs to be recognized by both. Low-density lipoprotein receptor-related protein-1 (LRP1) has been observed to express on both the BBB and glioma cells.[21−23]

Received: February 7, 2014
Revised: June 19, 2014
Accepted: June 24, 2014
Published: July 1, 2014

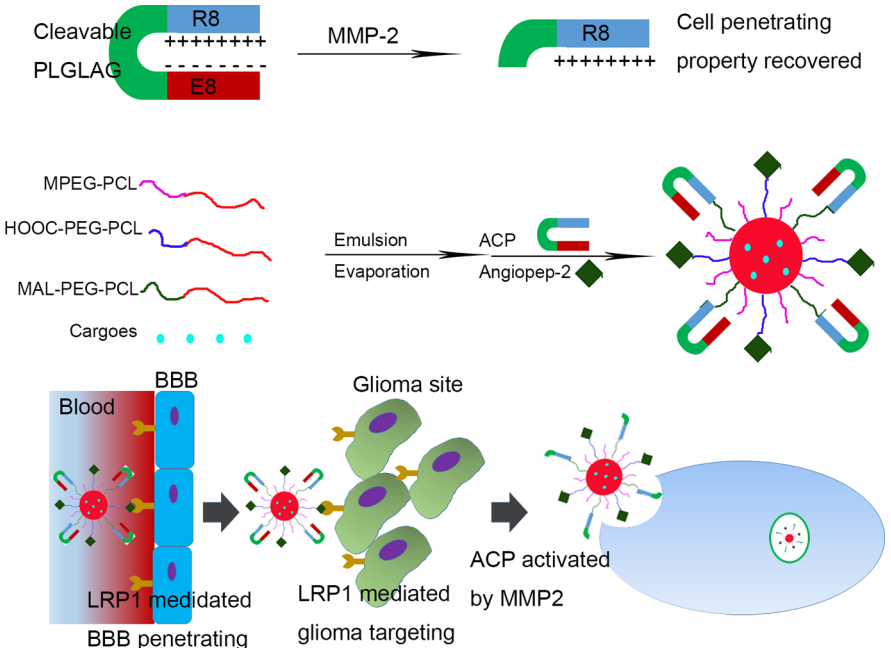

Figure 1. Elucidation of the study. The cell penetrating property could be activated by MMP-2. AnACNPs could transport through BBB and target to glioma because of angiopep-2 could bind with LRP1 that expressed on BBB and glioma cells. ACP could be activated in glioma site owing to the high expression level of MMP-2, which led to improved cell penetrating property.

Thus, the corresponding ligand could be used for dual-targeting delivery to the BBB and glioma cells. Angiopep-2, which is derived from the Kunitz domain of aprotinin, exhibits high LRP1 binding efficiency and has been used for glioma-targeting delivery by several research groups.[24−26] Thus, we used angiopep-2 in this study to enable the NPs to penetrate through the BBB and actively target glioma.

To improve the tissue penetration efficiency, NPs were functionalized with activatable CPP (ACP): EEEEEEEE(E8)-6-aminohexanoyl-PLGLAG-RRRRRRRR(R8). In the blood, cationic R8 is covered by E8 through electrostatic forces, and the penetration ability of R8 is shielded.[7] The expression level of matrix metalloproteinase (MMP)-2 is high in the glioma site, whereas PLGLAG is the substrate of MMP-2.[8,27] Thus, E8 could be detached from R8 at the glioma site, leading to a recovery of penetration ability of R8.

Docetaxel (DTX) is a taxane derivate that has been extensively applied for treating several malignant cancers including lung cancer, breast cancer, and ovarian cancer.[28,29] Although DTX inhibited the proliferation of glioma cells in vitro, it failed to show any benefit in the treatment of glioma patients, which was ascribed to the poor glioma-targeting ability and restriction provided by the BBB.[30,31] Therefore, we used DTX as a model drug to evaluate the glioma-targeting ability and treatment efficiency of the constructed delivery system.

In this study, in vitro and in vivo experiments were performed to explore the targeting delivery effect of angiopep-2 and ACP dual-modified NPs (AnACNPs). To monitor the in vitro and in vivo behaviors, coumarin-6 and DiR, two commonly used dyes, were loaded into the NPs. DTX was also loaded into the particles to evaluate the antiglioma effect of AnACNPs.

2. MATERIALS AND METHODS

Materials. Angiopep-2, ACP, and R8 were synthesized by Sangon Biotech (Shanghai, China). DTX was purchased from Knowshine (Shanghai, China). Methoxy poly(ethylene glycol)−poly(ε-caprolactone) (MPEG−PCL; M_w: 3k−15k), maleimide poly(ethylene glycol)−poly(ε-caprolactone) (MAL−PEG−PCL; M_w: 3.4k−15k), and carboxyl poly(ethylene glycol)−poly(ε-caprolactone) (HOOC−PEG−PCL; M_w: 3.4k−15k) were synthesized as previously described.[32] Coumarin-6, *N*-(3-(dimethylamino)propyl)-*N*′-ethylcarbodiimide hydrochloride (EDC) and *N*-hydroxysuccinimide (NHS) were obtained from Sigma (Saint Louis, MO, U. S. A.). DiR was obtained from Biotium (Hayward, CA, U. S. A.). Reagents for Western blot were purchased from Beyotime (Haimen, China). DTX was purchased from Knowshine (Shanghai, China). U-87 MG (from human), C6 (from rat), brain microvessel endothelial cells (BMEC, from rat), and A549 (from human) cell lines, as well as human umbilical vein endothelial cells (HUVEC) were obtained from the Institute of Biochemistry and Cell Biology, Shanghai Institutes for Biological Sciences, Chinese Academy of Sciences (Shanghai, China). A bEnd.3 cell line (from mouse) was obtained from the American Type Culture Collection (ATCC; Manassas, VA, U. S. A.). Plastic cell culture dishes and plates were purchased from Wuxi NEST Biotechnology Co. Ltd. (Wuxi, China). Dulbecco's modified Eagle's (high glucose) cell culture medium and fetal bovine serum were obtained from Life Technologies (Grand Island, NY, U. S. A.). 4,6-Diamidino-2-phenylindole (DAPI) was purchased from Beyotime (Haimen, China). Rabbit anti-MMP-2 antibody and rabbit anti-MMP-2 antibody were purchased from Abcam Ltd. (Hong Kong, China). Rabbit antiactin antibody was purchased from Santa Cruz Biotechnology, Inc. (Santa Cruz, CA, U. S. A.). Peroxidase-conjugated goat antirabbit secondary antibody was purchased from Jackson Immunoresearch Laboratories, Inc. (West Grove, PA, U. S. A.). All other chemicals were purchased from Sinopharm Chemical Reagent (Shanghai, China).

BALB/c mice and BALB/c nude mice (male, 4−5 weeks, 18−22 g) were obtained from the Shanghai Laboratory Animal

Center (SLAC) Co. Ltd. (Shanghai, China) and maintained under standard housing conditions. All animal experiments were performed following protocols evaluated and approved by the ethics committee of Fudan University.

Preparation and Characterization of NPs. PEG−PCL nanoparticles (NPs) were prepared using a previously described emulsion/solvent evaporation method.[33] In brief, 28 mg of MPEG−PCL, 1 mg of HOOC−PEG−PCL, and 1 mg of MAL−PEG−PCL were dissolved in 1 mL of dichloromethane and then added into 5 mL of a 0.6% sodium cholate hydrate solution. The mixture was then pulse-sonicated for 75 s at 200 W on ice using a probe sonicator (Scientz Biotechnology Co. Ltd., China). Subsequently, the emulsion was applied to a rotary evaporator to remove the dichloromethane, and the NPs were condensed to a fixed concentration by ultrafiltration at 4000*g*.

For the angiopep-2 conjugation (AnNPs), the carboxyl unit of the NPs was activated by EDC and NHS in a pH 6.0 MES buffer for 0.5 h. The MES buffer was then replaced with phosphate-buffered saline (PBS, pH 7.4) using a Hitrap desalting column. Subsequently, 50 μg of angiopep-2 in 1 mL of PBS (pH 7.4) was added into the NP suspension and stirred for 4 h in the dark. For the R8 or ACP conjugation (CNPs, ACNPs, and AnACNPs), 50 μg of R8 or ACP was added to the NP or AnNP suspension and stirred for 6 h in the dark. The product was then applied to a Sepharose CL-4B column to remove the unconjugated peptides, and the particles were collected. DTX-, coumarin-6- and DiR-loaded AnACNPs were prepared using the same procedure, but the materials were dissolved in 1 mL of dichloromethane, which contained 1 mg of DTX, 30 μg of coumarin-6, or 300 μg of DiR.

Particle size and zeta potential was determined by dynamic light scattering (DLS), using a Malvern Zetasizer (Malvern, NanoZS, U. K.). Particle morphology was detected using a transmission electron microscope (TEM; H-600, Hitachi, Japan) after negative staining with a 2% sodium phosphotungstate solution. The concentration of DTX in various NPs was determined by HPLC using previously established conditions.[34]

Protein Expression. HUVEC, bEnd.3, BMEC, C6, U-87 MG, and A549 cells were lysed using RIPA buffer containing 1 mM PMSF. The protein concentration was determined using the BCA method. Equivalent amounts of protein were boiled for 5 min in a loading buffer and then separated by 10% SDS polyacrylamide gel electrophoresis. Proteins were transferred to nitrocellulose membranes. The membranes were blocked for 1 h in TBS containing 4% low-fat milk. Membranes were then probed with rabbit anti-MMP-2 antibody (1:500), rabbit anti-LRP1 antibody (1:500), and rabbit antiactin antibody (1:1000) followed by peroxidase-conjugated goat antirabbit secondary antibody (1:1000) to recognize the target proteins. The proteins were visualized using an ECL reagent.

Cellular Uptake. To determine the function of the ACP, BMEC, and C6 cells in the logarithmic growth phase were seeded on 12-well plates at a density of 1×10^4 cells/mL. Twenty-four hours later, 100 μg/mL of coumarin-6-loaded NPs, CNPs, ACNPs, or batimastat (MMP-2/9 inhibitor)-containing ACNPs were added into the wells and incubated for 1 h. The adsorptive and free particles were removed by washing three times with ice-cold PBS. To quantitatively determine the fluorescence intensity, the cells were digested and detected using a FACSAria cell sorter (BD, U. S. A.). To determine the effect of modifications on cellular uptake, 100 μg/mL of coumarin-6-loaded formulations were added into C6 cell-seeded wells and incubated for 1 h. The fluorescence intensity of the cells was determined as previously described.

Antiproliferation Study. The cytotoxicity of various formulations was evaluated using a CCK-8 kit. C6 cells (2×10^4 cells/mL) were seeded in 96-well plates. Twenty-four hours later, DTX, DTX-loaded NPs, AnNPs, CNPs, ACNPs, or AnACNPs were added with serial concentrations from 10 μg of DTX/mL to 0.01 pg of DTX/mL. After 72 h, 10 μL of CCK-8 was added into each well. After 1 h, the absorption at 450 nm was detected using a microplate reader (Multiskan MK3, Thermo, U. S. A.).

Cell Apoptosis. Two days after being seeded in 6-well plates at a density of 10^5 cells/mL, C6 cells were treated with 0.5 μg/mL of DTX, DTX-loaded NPs, AnNPs, CNPs, ACNPs, or AnACNPs. Untreated cells were used as controls. After 24 h, cells were analyzed. For quantitative assays, cells were harvested by trypsinization, centrifuged at 1000 rpm for 3 min, and resuspended in a binding buffer. After adding 5 μL of both annexin V-FITC and propidium iodide (50 μg/mL), cells were incubated at room temperature for 5 min in the dark. Cell apoptosis was analyzed using a flow cytometer (BD, U. S. A.). For qualitative assays, cells were stained with Hoechst 33342 before observation with a fluorescence microscope (Leica, Germany). To further demonstrate the dual-targeting effect, BMEC were seeded in transwells at a density of 1×10^5 cells/well. The transendothelial electrical resistance (TEER) was recorded daily. When the TEER was sustained over 150 Ω, transwells were cocultured with C6-containing plates for 24 h. Subsequently, 0.5 μg/mL of different formulations were added into the transwells. After 24 h of incubation, the apoptosis of C6 cells was analyzed as previously described.

In Vivo Imaging. Glioma-bearing mice were established as previously described.[35] Mice were anesthetized and fixed on a stereotaxic apparatus. A 5-μL suspension containing 5×10^5 C6 cells was slowly injected into the right corpus striatum of the nude mice. Ten days later, 2 mg/kg of DiR-loaded NPs, CNPs, ACNPs, AnNPs, or AnACNPs were injected into the glioma-bearing mice. The distribution of fluorescence was observed using a spectrum in vivo imaging system (Caliper, MA, U. S. A.), 2 and 24 h after injection. Mice were sacrificed at 24 h, and the ex vivo images of the brains were also captured at that time.

Glioma Distribution. Glioma-bearing mice were established as previously described, except that C6 cells were replaced with RFP-C6 cells. Twelve days after tumor implantation, the coumarin-6-loaded NPs, AnNPs, ACNPs, CNPs, or AnACNPs were intravenously (iv) administered to the mice. After 2 h, the mice were anesthetized, and the hearts were perfused with saline, followed by 4% paraformaldehyde. The brains were removed for consecutively preparing 5-μm-thick frozen sections. Nuclei were stained with 1 μg/mL of DAPI for 5 min. The distribution of fluorescence was observed using a confocal microscope (TCS SP5, Leica, Germany).

Antiglioma Effect. The orthotopic glioma-bearing mice were established as previously described. Eight days after cell injections, the nude mice were randomly divided into the following six groups (10 mice per group): a saline group, DTX-NP group, DTX-CNP group, DTX-ACNP group, DTX-AnNP group, and DTX-AnACNP group. Each mouse received a dose of 6 mg/kg four times every 3 days. Survival time was recorded and analyzed using SPSS 10.0 (IBM, U. S. A.).

Statistical Analysis. Data were presented as means ± SD. Statistical differences in cellular uptake, cellular apoptosis, and in vivo imaging were determined using the Student's *t* test. The

probability of survival was determined using the Kaplan−Meier method and compared using the log-rank test.

3. RESULTS

Characterization. The particle size of AnACNPs was approximately 110 nm, with a narrow distribution (PDI < 0.3, Figure 2 A, Table 1). The AnACNPs were mostly spherical according to TEM (Figure 2 B). The zeta potentials of all types of particles were approximately −5 mV.

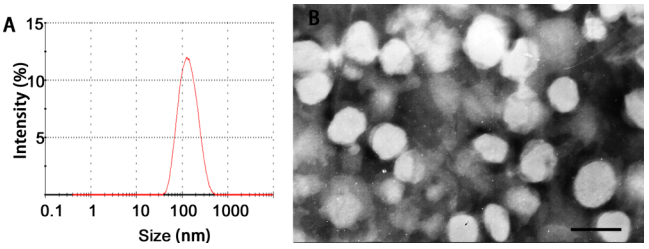

Figure 2. (A) Size distribution of AnACNPs determined by DLS. (B) Morphology of AnACNPs captured by TEM; the bar represents 100 nm.

Table 1. Particle Size and Zeta Potential of Different Nanoparticles

formulations	particle size (nm)	PDI	zeta potential (mV)
NPs	105.4	0.179	−6.73
CNPs	110.3	0.217	−0.47
ACNPs	112.9	0.206	−7.41
AnNPs	108.4	0.194	−6.18
AnACNPs	115.3	0.228	−6.72

Protein Expression. The expression of LRP1 and MMP-2 was evaluated on several cells (Supporting Information Figure S1). The LRP1 expression levels on tumor cells, BMEC, and bEnd.3 cells (normally used as a simple model of the BBB) were considerably high, suggesting that LRP1 could be used as a target for dual-targeting delivery in brain tumors. The high MMP-2 expression on glioma cells (U-87 MG) was consistent with that reported in other studies.

Cellular Uptake. To evaluate the function of ACP, cellular uptake experiments were performed on both BMEC and C6 cells, using CNPs as the control and batimastat as the inhibitor of MMP-2/9 (Figure 3 A). ACP and R8 modification increased the cellular uptake by both BMEC and C6 cells, which was consistent with the results of MMP-2 expression experiments. However, adding batimastat substantially decreased the cellular uptake of ACNPs. No substantial difference was observed between the NP group and ACNP + batimastat group, suggesting that ACP could not boost the cell-penetrating property without MMP-2/9, which was useful for decreasing the normal tissue distribution. C6 cells were used to evaluate the uptake behavior of different formulations (Figure 3 B). Angiopep-2 modification increased the cellular uptake, which was consistent with the high LRP1 expression on C6 cells. Dual modification with angiopep-2 and ACP further improved the C6 uptake, demonstrating its superiority in delivering cargoes to cells.

Antiproliferation Study. DTX was loaded into formulations to evaluate its cytotoxicity on C6 cells (Figure 4). 50%

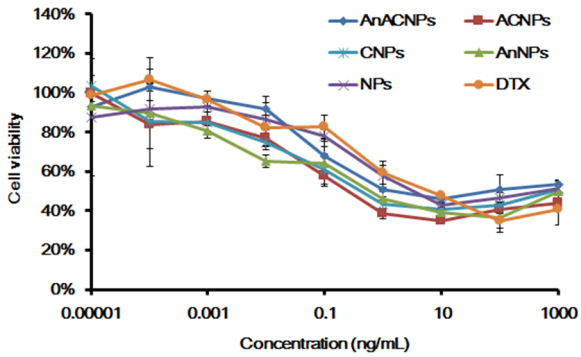

Figure 4. Antiproliferation effect of different formulations at a serial concentrations against C6 cells; $n = 3$.

inhibiting concentration (IC_{50}) values of 7.52 ng/mL, 5.7 ng/mL, 1.18 ng/mL, 2.17 ng/mL, 1.36 ng/mL, and 1.03 ng/mL were obtained for DTX, NPs, ACNPs, CNPs, AnNPs, and AnACNPs, respectively. Although DTX and DTX-NPs effectively inhibited the proliferation of C6 cells, modification with R8, ACP, angiopep-2, and dual modification with ACP and angiopep-2 further boosted this effect, probably because of the enhanced cellular uptake, as previously demonstrated.

Cell Apoptosis. To further evaluate the effect of different formulations, cell apoptosis experiments were performed. Traditionally, formulations were directly added into cancer cell-seeded plates or dishes. Substantially more apoptotic cells than control cells were induced by DTX and DTX-NPs at a concentration of 0.5 μg/mL (Figure 5 A, Supporting

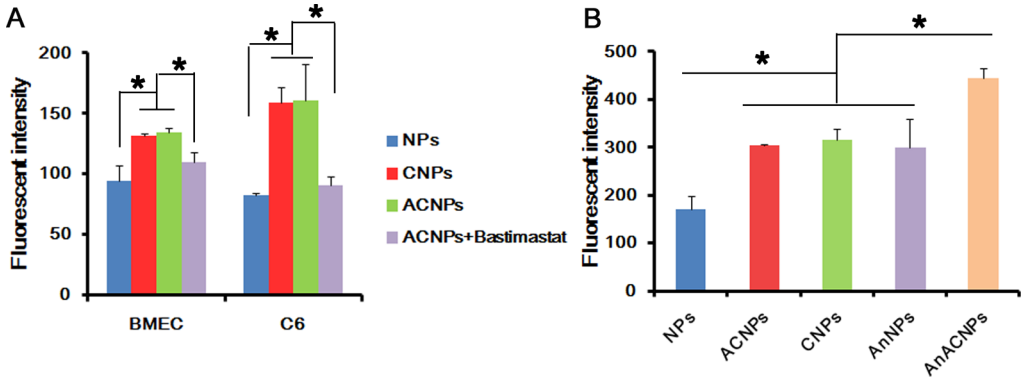

Figure 3. Cellular uptake manners. (A) BMEC and C6 cells uptake of NPs, CNPs, ACNPs without/with batimastat. (B) C6 cell uptake of different formulations; $n = 3$, $^*p < 0.05$.

dx.doi.org/10.1021/mp500113p | Mol. Pharmaceutics 2014, 11, 2755−2763

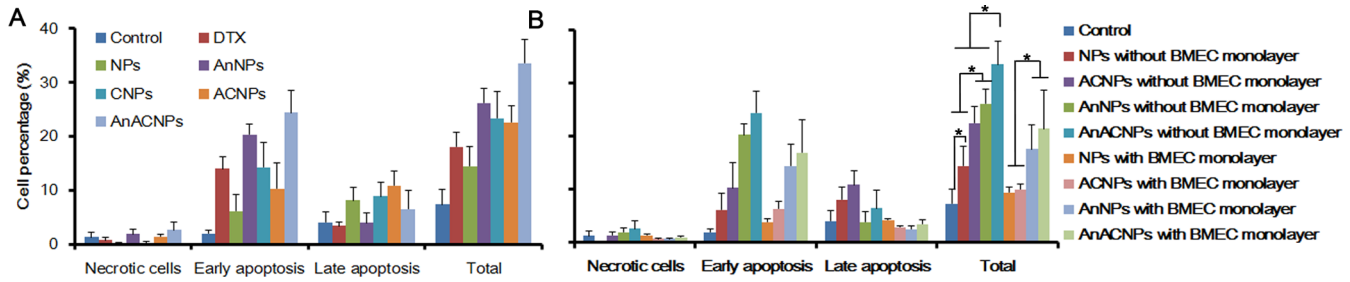

Figure 5. (A) C6 cell apoptosis induced by 0.5 μg/mL different formulations. (B) Cell apoptosis induced by 0.5 μg/mL different formulations on C6 cells with or without BMEC monolayers; $n = 3$, $^*p < 0.05$.

Information Figure S2). NPs modified with ACP, R8, or angiopep-2 effectively boosted the apoptosis induction effect, which induced substantially more apoptotic cells than did DTX-NPs, owing to the high cellular uptake ability, as demonstrated by the cellular uptake study. Dual modification with ACP and angiopep-2 further improved the cellular uptake; thus, DTX-AnACNPs induced the highest percentages of apoptotic cells among all treatments, which was consistent with the result of cytotoxicity experiments.

However, to be able to reach cancers in vivo, particularly brain cancers, formulations need to overcome several barriers. To mimic this microenvironment, we cocultured C6 cells with a BMEC cell monolayer. Formulations were added into transwells, and the apoptosis of C6 cells in receiving wells was detected. Although DTX-ACNPs induced a higher percentage of apoptotic cells than did DTX-NPs when directly added onto C6 cells, no difference between DTX-ACNPs and DTX-NPs was observed in the cocultured systems (Figure 5 B, Supporting Information Figure S2), suggesting that ACP modification facilitated the cellular uptake of the C6 cells rather than that of BMEC, which agreed with the results of cellular uptake experiments. Because of the high LRP1 expression on both BMEC and C6 cells, angiopep-2 modification induced a substantially higher percentage of apoptotic cells than did DTX-NPs in C6 cells, both with and without BMEC monolayers. Dual modification with ACP and angiopep-2 further boosted the apoptotic induction effect, suggesting that dual modification could be useful to overcome barriers for treating brain glioma.

In Vivo Imaging. Different formulations presented diverse targeting effects (Figure 6). Two hours after administration, unmodified NPs and CNPs were rarely distributed in the brain, whereas ACNPs, AnNPs, and AnACNPs exhibited an obviously high intensity in the brain. After increasing the period to 24 h, the distribution of all formulations in the brain also increased. However, NPs and CNPs still exhibited the lowest intensity in the brain, compared with other nanoparticles, owing to the poor targeting effect of NPs and intensive systemic distribution of CNPs. AnNPs exhibited a higher concentration in the brain than that of NPs and CNPs, suggesting that angiopep-2 could be effectively transported through the BBB, and targeted the brain glioma because of the high expression level of LRP1 on both the BBB and glioma cells, which agreed with previous studies. The cell-penetrating property of ACP was hindered in the blood and recovered in the glioma site because of the high expression level of MMP-2, resulting in a higher distribution of ACNPs in the glioma than that of NPs and CNPs. By combining the specific targeting effect of angiopep-2 and activatable cell-penetrating property of ACP, AnACNPs exhibited the highest concentration in the glioma. The targeting

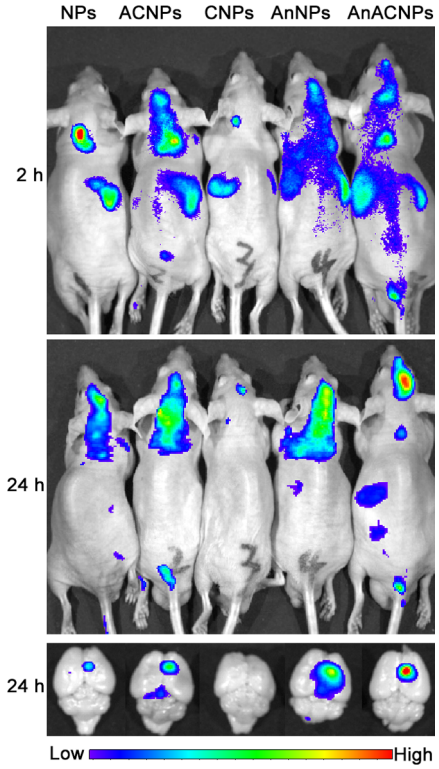

Figure 6. In vivo imaging of whole body and ex vivo imaging of brain from mice that treated with different DiR-loaded formulations.

effect of different formulations was further demonstrated by ex vivo imaging of brain.

Glioma Distribution. To elucidate the distribution of particles in glioma-bearing brains, frozen sections were prepared and nuclei were stained (Figure 7). A low NP intensity was observed in the glioma site, which was due to the poor targeting efficiency. The fluorescence intensity in the brains from CNP-treated mice was low, because of the high distribution in the whole body. AnNPs targeted both the BBB and glioma cells, resulting in a considerably high localization in the glioma, which was consistent with other studies. The fluorescence intensity of cells from ACNP-treated mice was higher than that of cells from NP- and CNP-treated mice because of the activatable cell-penetrating property of ACP, which resulted in a glioma-specific enhanced cell penetration. By combining the effect of angiopep-2 and ACP, AnACNPs exhibited the highest localization in the glioma site, suggesting that dual modification improved the glioma-targeting efficiency, which was useful for treating the glioma.

dx.doi.org/10.1021/mp500113p | Mol. Pharmaceutics 2014, 11, 2755−2763

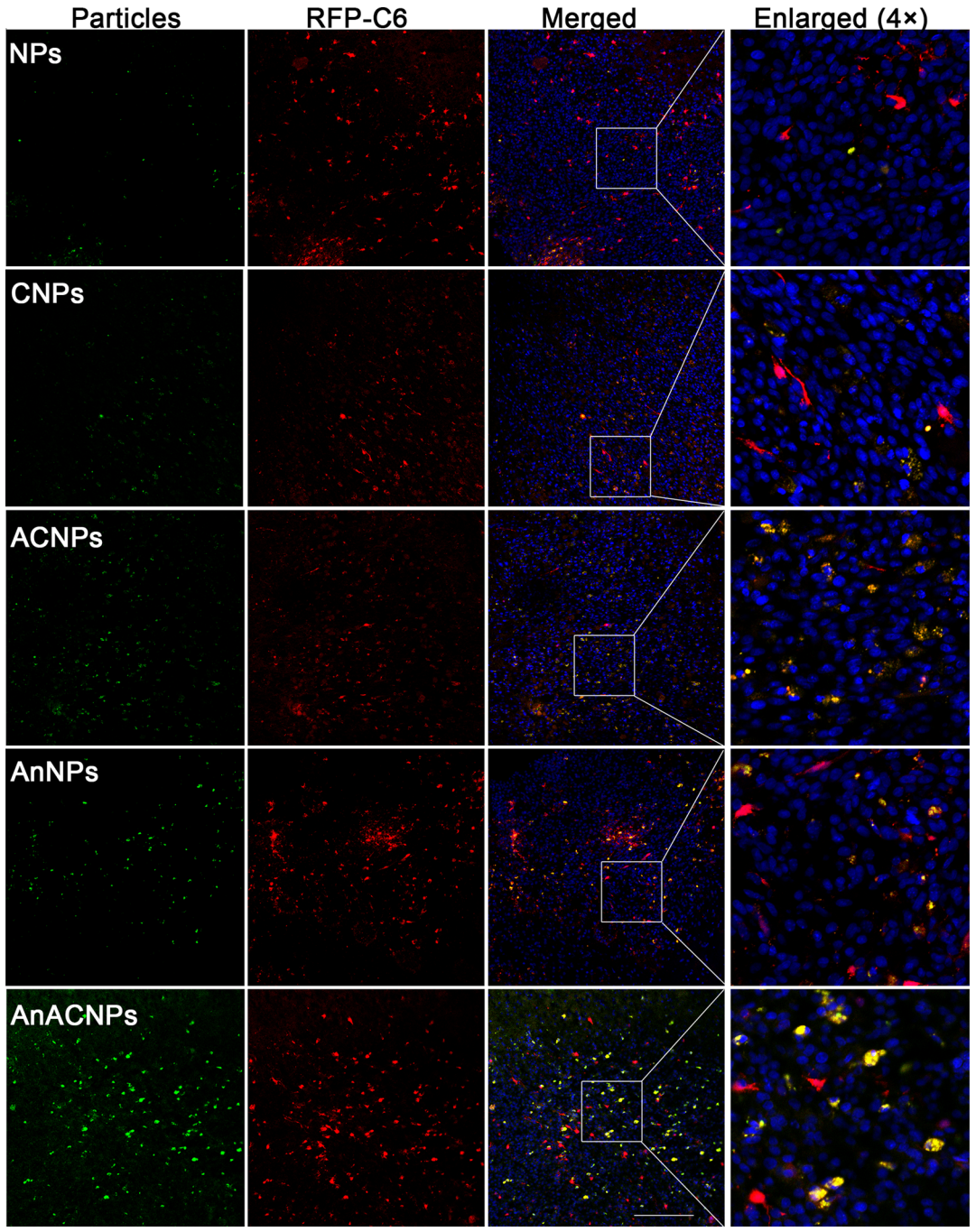

Figure 7. Distribution of vary particles in brain tumor. Nuclei were stained by DAPI, particles were marked with coumarin-6, and brain tumor cells were RFP-C6. The bar was 200 μm.

In Vivo Antiglioma Effect. To evaluate the antiglioma effect of the dual-targeting delivery systems, DTX was loaded into different types of particle (Figure 8). Although DTX-NPs expanded the median survival time from 19 days to 20 days, no statistical difference was observed between the DTX-NP group and saline group, which may be explained by the poor glioma-targeting efficiency of NPs. Because of the poor glioma-targeting effect and intensive systemic distribution, the median survival time of the DTX-CNP group was only 16 days, which was even shorter than that of the saline group. Treatment with AnNPs and ACNPs significantly prolonged the median survival time because of the glioma-targeting effect of AnNPs and ACNPs, which was 1.42- and 1.37-fold higher than that of saline. Dual modification with angiopep-2 and ACP further improved the treatment outcome because of the dual-targeting effect of AnACNPs, which was demonstrated by in vivo imaging. The median survival time of mice treated with DTX-AnACNPs was 1.68-fold higher than that of mice treated with saline, which in turn was substantially higher than that of DTX-AnNP- and DTX-ACNP-treated mice.

4. DISCUSSION AND CONCLUSION

To improve the treatment outcome of glioma, dual-targeting delivery systems were developed to overcome two barriers: the BBB and BTB.[36] Normally, delivery systems are anchored to a BBB-targeting ligand and a glioma cell-targeting ligand to

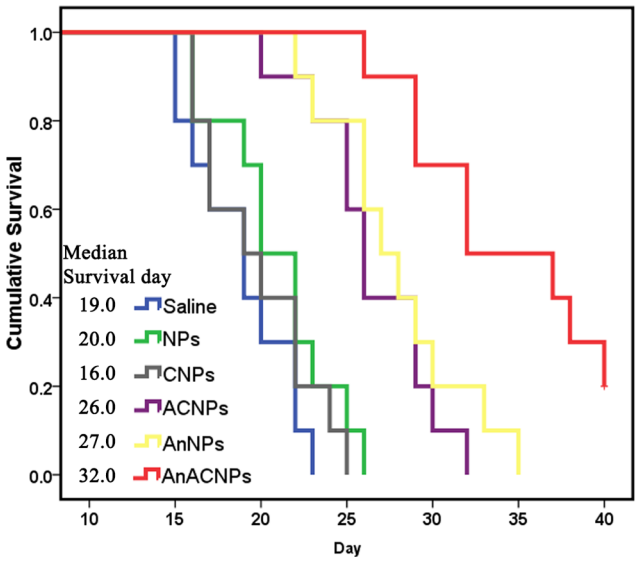

Figure 8. Survival curve of the brain glioma bearing mice treated with different formulations of the same dose; $n = 10$.

mediate the systems specifically targeted to glioma cells. For example, TGN peptide- and AS1411 aptamer-modified NPs exhibit a precise glioma-targeting property because of the BBB-targeting property of TGN and glioma-targeting property of the AS1411 aptamer.[19] In addition, some receptors, such as the transferrin receptor and LRP1, are highly expressed on both the BBB and glioma cells,[21,22,37,38] which was also confirmed by the current study. The corresponding ligands could be used for dual-targeting delivery. In this study, angiopep-2 was used for glioma-targeting delivery. Both in vitro cellular uptake and in vivo imaging demonstrated that conjugating with angiopep-2 boosts the glioma cellular uptake and glioma accumulation of NPs, agreeing with previous studies.[20,25] Some studies have demonstrated that angiopep-2-modified NPs or micelles could target not only glioma-bearing brains but also healthy brains, thus proving the dual-targeting efficiency of angiopep-2.[24,39−41]

However, penetration ability is crucial for delivery systems transporting drugs into glioma cells that are distant from microvessels. Thus, CPP modification is essential for improving the glioma-targeting drug delivery. Furthermore, the saturation of receptor-mediated endocytosis intensifies the need for CPP modification.[42−44] To circumvent their poor selectivity, CPPs could be covered with PEG or anionic peptides through environment-sensitive bonds such as acidic-, reductive-, and protease-sensitive bonds.[45−47] In this study, E8 was used to hinder the cationic property of R8 through an MMP-2/9-sensitive linker. The results demonstrated that the cell-penetrating property of ACP was almost the same as that of CP, suggesting that E8 was almost completely detached. The cell-penetrating property of ACP was covered because the uptake of ACNPs in the presence of batimastat was almost the same as that of NPs, which was consistent with previous studies.[46] Because the cell-penetrating property was improved, the distribution of ACNPs in normal tissues was lower than that of CNPs, suggesting that the cell-penetrating property of ACP was recovered in tumors, enhancing the glioma-penetrating ability of ACNPs and AnACNPs. Thus, DTX-loaded AnACNPs exhibited the most favorable antiglioma effect.

Several studies have used ACPs and a specific ligand for dual-targeting delivery.[42,43,48−52] Most studies have reported an enhanced tumor-targeting delivery and antitumor effect. However, most studies have focused on peripheral tumors rather than brain tumors, and to the best of our knowledge, this is the first time the combination of the dual brain glioma-targeting delivery by a specific ligand and elevated tumor penetration by ACP has been reported. Although the current strategy exhibits an effective glioma-targeting delivery and antiglioma effect, several aspects could be improved. First, dual modification is complex. Chimeric peptides exhibiting a specific targeting sequence and cell-penetrating sequence may be the future direction of dual-targeting delivery.[43] Second, the proportion of two ligands needs to be optimized. Although a high ligand concentration can facilitate internalization by specific cells, it also tends to activate the immune system or the recognition by the reticuloendothelial system, resulting in rapid blood clearance and high liver accumulation.[32]

In conclusion, a novel drug delivery system was developed for glioma dual targeting and increased glioma penetration. The results demonstrated that the system effectively targeted gliomas, and attained a substantial antiglioma effect.

■ ASSOCIATED CONTENT

Supporting Information

Protein expression on different cells and flow cytometry dot-plot imaging. This material is available free of charge via the Internet at http://pubs.acs.org.

■ AUTHOR INFORMATION

Corresponding Author

*X. Jiang. Phone: +86-21-51980067. E-mail: xgjiang@shmu.edu.cn.

Notes

The authors declare no competing financial interest.

■ ACKNOWLEDGMENTS

This work was supported by the National Basic Research Program of China (973 Program, 2013CB932502) and National Science and Technology Major Project (2012ZX09304004).

■ REFERENCES

(1) Matsumura, Y.; Maeda, H. A new concept for macromolecular therapeutics in cancer chemotherapy: mechanism of tumoritropic accumulation of proteins and the antitumor agent smancs. *Cancer Res.* **1986**, *46*, 6387−6392.

(2) Fang, J.; Nakamura, H.; Maeda, H. The EPR effect: Unique features of tumor blood vessels for drug delivery, factors involved, and limitations and augmentation of the effect. *Adv. Drug Delivery Rev.* **2011**, *63*, 136−151.

(3) Foged, C.; Nielsen, H. M. Cell-penetrating peptides for drug delivery across membrane barriers. *Expert Opin. Drug Delivery* **2008**, *5*, 105−117.

(4) Marcucci, F.; Lefoulon, F. Active targeting with particulate drug carriers in tumor therapy: fundamentals and recent progress. *Drug Discovery Today* **2004**, *9*, 219−228.

(5) Kondo, E.; Saito, K.; Tashiro, Y.; Kamide, K.; Uno, S.; Furuya, T.; Mashita, M.; Nakajima, K.; Tsumuraya, T.; Kobayashi, N.; Nishibori, M.; Tanimoto, M.; Matsushita, M. Tumour lineage-homing cell-penetrating peptides as anticancer molecular delivery systems. *Nat. Commun.* **2012**, *3*, 951.

(6) Alberici, L.; Roth, L.; Sugahara, K. N.; Agemy, L.; Kotamraju, V. R.; Teesalu, T.; Bordignon, C.; Traversari, C.; Rizzardi, G. P.;

Ruoslahti, E. De novo design of a tumor-penetrating peptide. *Cancer Res.* **2013**, *73*, 804−812.
(7) Jiang, T.; Olson, E. S.; Nguyen, Q. T.; Roy, M.; Jennings, P. A.; Tsien, R. Y. Tumor imaging by means of proteolytic activation of cell-penetrating peptides. *Proc. Natl. Acad. Sci. U. S. A.* **2004**, *101*, 17867−17872.
(8) Olson, E. S.; Jiang, T.; Aguilera, T. A.; Nguyen, Q. T.; Ellies, L. G.; Scadeng, M.; Tsien, R. Y. Activatable cell penetrating peptides linked to nanoparticles as dual probes for in vivo fluorescence and MR imaging of proteases. *Proc. Natl. Acad. Sci. U. S. A.* **2010**, *107*, 4311−4316.
(9) Kuai, R.; Yuan, W.; Li, W.; Qin, Y.; Tang, J.; Yuan, M.; Fu, L.; Ran, R.; Zhang, Z.; He, Q. Targeted delivery of cargoes into a murine solid tumor by a cell-penetrating peptide and cleavable poly(ethylene glycol) comodified liposomal delivery system via systemic administration. *Mol. Pharmaceutics* **2011**, *8*, 2151−2161.
(10) Pardridge, W. M. Vector-mediated drug delivery to the brain. *Adv. Drug Delivery Rev.* **1999**, *36*, 299−321.
(11) Gaillard, P. J.; Visser, C. C.; de Boer, A. G. Targeted delivery across the blood-brain barrier. *Expert Opin. Drug Delivery* **2005**, *2*, 299−309.
(12) Terasaki, T.; Hosoya, K. The blood-brain barrier efflux transporters as a detoxifying system for the brain. *Adv. Drug Delivery Rev.* **1999**, *36*, 195−209.
(13) Wolburg, H.; Noell, S.; Fallier-Becker, P.; Mack, A. F.; Wolburg-Buchholz, K. The disturbed blood-brain barrier in human glioblastoma. *Mol. Aspects Med.* **2012**, *33*, 579−589.
(14) Agarwal, S.; Sane, R.; Oberoi, R.; Ohlfest, J. R.; Elmquist, W. F. Delivery of molecularly targeted therapy to malignant glioma, a disease of the whole brain. *Expert Rev. Mol. Med.* **2011**, *13*, e17.
(15) Bronger, H.; Konig, J.; Kopplow, K.; Steiner, H. H.; Ahmadi, R.; Herold-Mende, C.; Keppler, D.; Nies, A. T. ABCC drug efflux pumps and organic anion uptake transporters in human gliomas and the blood-tumor barrier. *Cancer Res.* **2005**, *65*, 11419−11428.
(16) Groothuis, D. R. The blood-brain and blood-tumor barriers: a review of strategies for increasing drug delivery. *Neuro-Oncology* **2000**, *2*, 45−59.
(17) Roberts, W. G.; Delaat, J.; Nagane, M.; Huang, S.; Cavenee, W. K.; Palade, G. E. Host microvasculature influence on tumor vascular morphology and endothelial gene expression. *Am. J. Pathol.* **1998**, *153*, 1239−1248.
(18) Zhan, C.; Lu, W. The blood-brain/tumor barriers: challenges and chances for malignant gliomas targeted drug delivery. *Curr. Pharm. Biotechnol.* **2012**, *13*, 2380−2387.
(19) Gao, H.; Qian, J.; Cao, S.; Yang, Z.; Pang, Z.; Pan, S.; Fan, L.; Xi, Z.; Jiang, X.; Zhang, Q. Precise glioma targeting of and penetration by aptamer and peptide dual-functioned nanoparticles. *Biomaterials* **2012**, *33*, 5115−5123.
(20) Xin, H.; Jiang, X.; Gu, J.; Sha, X.; Chen, L.; Law, K.; Chen, Y.; Wang, X.; Jiang, Y.; Fang, X. Angiopep-conjugated poly(ethylene glycol)-co-poly(epsilon-caprolactone) nanoparticles as dual-targeting drug delivery system for brain glioma. *Biomaterials* **2011**, *32*, 4293−4305.
(21) Maletinska, L.; Blakely, E. A.; Bjornstad, K. A.; Deen, D. F.; Knoff, L. J.; Forte, T. M. Human glioblastoma cell lines: levels of low-density lipoprotein receptor and low-density lipoprotein receptor-related protein. *Cancer Res.* **2000**, *60*, 2300−2303.
(22) Ito, S.; Ohtsuki, S.; Terasaki, T. Functional characterization of the brain-to-blood efflux clearance of human amyloid-beta peptide (1−40) across the rat blood-brain barrier. *Neurosci. Res.* **2006**, *56*, 246−252.
(23) Demeule, M.; Currie, J. C.; Bertrand, Y.; Che, C.; Nguyen, T.; Regina, A.; Gabathuler, R.; Castaigne, J. P.; Beliveau, R. Involvement of the low-density lipoprotein receptor-related protein in the transcytosis of the brain delivery vector angiopep-2. *J. Neurochem.* **2008**, *106*, 1534−1544.
(24) Shao, K.; Huang, R.; Li, J.; Han, L.; Ye, L.; Lou, J.; Jiang, C. Angiopep-2 modified PE-PEG based polymeric micelles for amphotericin B delivery targeted to the brain. *J. Controlled Release* **2010**, *147*, 118−126.
(25) Huang, S.; Li, J.; Han, L.; Liu, S.; Ma, H.; Huang, R.; Jiang, C. Dual targeting effect of Angiopep-2-modified, DNA-loaded nanoparticles for glioma. *Biomaterials* **2011**, *32*, 6832−6838.
(26) Che, C.; Yang, G.; Thiot, C.; Lacoste, M. C.; Currie, J. C.; Demeule, M.; Regina, A.; Beliveau, R.; Castaigne, J. P. New Angiopep-modified doxorubicin (ANG1007) and etoposide (ANG1009) chemotherapeutics with increased brain penetration. *J. Med. Chem.* **2010**, *53*, 2814−2824.
(27) Forsyth, P. A.; Wong, H.; Laing, T. D.; Rewcastle, N. B.; Morris, D. G.; Muzik, H.; Leco, K. J.; Johnston, R. N.; Brasher, P. M.; Sutherland, G.; Edwards, D. R. Gelatinase-A (MMP-2), gelatinase-B (MMP-9) and membrane type matrix metalloproteinase-1 (MT1-MMP) are involved in different aspects of the pathophysiology of malignant gliomas. *Br. J. Cancer* **1999**, *79*, 1828−1835.
(28) Trudeau, M. E. Docetaxel: a review of its pharmacology and clinical activity. *Can. J. Oncol.* **1996**, *6*, 443−457.
(29) Lyseng-Williamson, K. A.; Fenton, C. Docetaxel: a review of its use in metastatic breast cancer. *Drugs* **2005**, *65*, 2513−2531.
(30) Sampath, P.; Rhines, L. D.; DiMeco, F.; Tyler, B. M.; Park, M. C.; Brem, H. Interstitial docetaxel (taxotere), carmustine and combined interstitial therapy: a novel treatment for experimental malignant glioma. *J. Neuro-Oncol.* **2006**, *80*, 9−17.
(31) Kemper, E. M.; Verheij, M.; Boogerd, W.; Beijnen, J. H.; van Tellingen, O. Improved penetration of docetaxel into the brain by co-administration of inhibitors of P-glycoprotein. *Eur. J. Cancer* **2004**, *40*, 1269−1274.
(32) Pang, Z.; Lu, W.; Gao, H.; Hu, K.; Chen, J.; Zhang, C.; Gao, X.; Jiang, X.; Zhu, C. Preparation and brain delivery property of biodegradable polymersomes conjugated with OX26. *J. Controlled Release* **2008**, *128*, 120−127.
(33) Gao, H.; Pan, S.; Yang, Z.; Cao, S.; Chen, C.; Jiang, X.; Shen, S.; Pang, Z.; Hu, Y. A cascade targeting strategy for brain neuroglial cells employing nanoparticles modified with angiopep-2 peptide and EGFP-EGF1 protein. *Biomaterials* **2011**, *32*, 8669−8675.
(34) Gao, H.; Pang, Z.; Pan, S.; Cao, S.; Yang, Z.; Chen, C.; Jiang, X. Anti-glioma effect and safety of docetaxel-loaded nanoemulsion. *Arch. Pharm. Res.* **2012**, *35*, 333−341.
(35) Jones-Bolin, S.; Zhao, H.; Hunter, K.; Klein-Szanto, A.; Ruggeri, B. The effects of the oral, pan-VEGF-R kinase inhibitor CEP-7055 and chemotherapy in orthotopic models of glioblastoma and colon carcinoma in mice. *Mol. Cancer Ther.* **2006**, *5*, 1744−1753.
(36) Gao, H.; Pang, Z.; Jiang, X. Targeted delivery of nano-therapeutics for major disorders of the central nervous system. *Pharm. Res.* **2013**, *30*, 2485−2498.
(37) Li, H.; Qian, Z. M. Transferrin/transferrin receptor-mediated drug delivery. *Med. Res. Rev.* **2002**, *22*, 225−250.
(38) Guo, L.; Ren, J.; Jiang, X. Perspectives on brain-targeting drug delivery systems. *Curr. Pharm. Biotechnol.* **2012**, *13*, 2310−2318.
(39) Thomas, F. C.; Taskar, K.; Rudraraju, V.; Goda, S.; Thorsheim, H. R.; Gaasch, J. A.; Mittapalli, R. K.; Palmieri, D.; Steeg, P. S.; Lockman, P. R.; Smith, Q. R. Uptake of ANG1005, a novel paclitaxel derivative, through the blood-brain barrier into brain and experimental brain metastases of breast cancer. *Pharm. Res.* **2009**, *26*, 2486−2494.
(40) Xin, H.; Sha, X.; Jiang, X.; Chen, L.; Law, K.; Gu, J.; Chen, Y.; Wang, X.; Fang, X. The brain targeting mechanism of Angiopep-conjugated poly(ethylene glycol)-co-poly(varepsilon-caprolactone) nanoparticles. *Biomaterials* **2012**, *33*, 1673−1681.
(41) Yan, H.; Wang, L.; Wang, J.; Weng, X.; Lei, H.; Wang, X.; Jiang, L.; Zhu, J.; Lu, W.; Wei, X.; Li, C. Two-Order Targeted Brain Tumor Imaging by Using an Optical/Paramagnetic Nanoprobe across the Blood Brain Barrier. *ACS Nano* **2012**, *6*, 410−420.
(42) Sharma, G.; Modgil, A.; Sun, C.; Singh, J. Grafting of cell-penetrating peptide to receptor-targeted liposomes improves their transfection efficiency and transport across blood-brain barrier model. *J. Pharm. Sci.* **2012**, *101*, 2468−2478.
(43) Sharma, G.; Modgil, A.; Layek, B.; Arora, K.; Sun, C.; Law, B.; Singh, J. Cell penetrating peptide tethered bi-ligand liposomes for

delivery to brain in vivo: Biodistribution and transfection. *J. Controlled Release* **2013**, *167*, 1−10.
(44) Kibria, G.; Hatakeyama, H.; Ohga, N.; Hida, K.; Harashima, H. Dual-ligand modification of PEGylated liposomes shows better cell selectivity and efficient gene delivery. *J. Controlled Release* **2011**, *153*, 141−148.
(45) Kuai, R.; Yuan, W.; Qin, Y.; Chen, H.; Tang, J.; Yuan, M.; Zhang, Z.; He, Q. Efficient Delivery of Payload into Tumor Cells in a Controlled Manner by TAT and Thiolytic Cleavable PEG Co-Modified Liposomes. *Mol. Pharm.* **2010**, 1816−1826.
(46) Gu, G.; Xia, H.; Hu, Q.; Liu, Z.; Jiang, M.; Kang, T.; Miao, D.; Tu, Y.; Pang, Z.; Song, Q.; Yao, L.; Chen, H.; Gao, X.; Chen, J. PEG-co-PCL nanoparticles modified with MMP-2/9 activatable low molecular weight protamine for enhanced targeted glioblastoma therapy. *Biomaterials* **2013**, *34*, 196−208.
(47) Huang, S.; Shao, K.; Kuang, Y.; Liu, Y.; Li, J.; An, S.; Guo, Y.; Ma, H.; He, X.; Jiang, C. Tumor targeting and microenvironment-responsive nanoparticles for gene delivery. *Biomaterials* **2013**, *34*, 5294−5302.
(48) Gao, W.; Xiang, B.; Meng, T. T.; Liu, F.; Qi, X. R. Chemotherapeutic drug delivery to cancer cells using a combination of folate targeting and tumor microenvironment-sensitive polypeptides. *Biomaterials* **2013**, *34*, 4137−4149.
(49) Jiang, T.; Zhang, Z.; Zhang, Y.; Lv, H.; Zhou, J.; Li, C.; Hou, L.; Zhang, Q. Dual-functional liposomes based on pH-responsive cell-penetrating peptide and hyaluronic acid for tumor-targeted anticancer drug delivery. *Biomaterials* **2012**, *33*, 9246−9258.
(50) Karagiannis, E. D.; Alabi, C. A.; Anderson, D. G. Rationally designed tumor-penetrating nanocomplexes. *ACS Nano* **2012**, *6*, 8484−8487.
(51) Kibria, G.; Hatakeyama, H.; Ohga, N.; Hida, K.; Harashima, H. Dual-ligand modification of PEGylated liposomes shows better cell selectivity and efficient gene delivery. *J. Controlled Release* **2011**, *153*, 141−148.
(52) Jiang, Q. Y.; Lai, L. H.; Shen, J.; Wang, Q. Q.; Xu, F. J.; Tang, G. P. Gene delivery to tumor cells by cationic polymeric nanovectors coupled to folic acid and the cell-penetrating peptide octaarginine. *Biomaterials* **2011**, *32*, 7253−7262.